Article

High pressure study of the organic compound $(TMTTF)_2BF_4$

RUETSCHI, Anna-Sabina, JACCARD, Didier

Abstract

High pressure resistivity measurements of the organic compound (TMTTF)2BF4 have been performed in a newly developped Bridgman cell providing good pressure conditions on a wide pressure range. For the first time in this compound a zero resistance superconducting state is observed between 3 and 4GPa. At temperatures above the superconducting transition, the resistivities of the two high quality samples show a different behavior. One sample, provides indications for a magnetic quantum critical point at the maximum of Tc, whereas in the other antiferromagnetic spin-fluctuations are present above Tc.

Reference

RUETSCHI, Anna-Sabina, JACCARD, Didier. High pressure study of the organic compound $(TMTTF)_2BF_4$. *The European physical journal. B, Condensed matter physics*, 2009, vol. 67, no. 1, p. 43-49

DOI : 10.1140/epjb/e2009-00006-x

Eur. Phys. J. B **67**, 43–49 (2009)
DOI: 10.1140/epjb/e2009-00006-x

THE EUROPEAN PHYSICAL JOURNAL B

Regular Article

High pressure study of the organic compound $(TMTTF)_2BF_4$

A.-S. Rüetschi[a] and D. Jaccard

DPMC, University of Geneva, 24 quai Ernest-Ansermet, 1211 Genève 4, Switzerland

Received 8 September 2008 / Received in final form 26 November 2008
Published online 9 January 2009

Abstract. High pressure resistivity measurements of the organic compound $(TMTTF)_2BF_4$ have been performed in a newly developped Bridgman cell providing good pressure conditions on a wide pressure range. For the first time in this compound a zero resistance superconducting state is observed between 3 and 4 GPa. At temperatures above the superconducting transition, the resistivities of the two high quality samples show a different behavior. One sample, provides indications for a magnetic quantum critical point at the maximum of T_c, whereas in the other antiferromagnetic spin-fluctuations are present above T_c.

PACS. 74.70.Kn Organic superconductors – 74.62.Fj Pressure effects

1 Introduction

Fabre and Bechgaard salts, short $(TM)_2X$, are isostructural compounds formed by stacks of a flat organic molecule (tetramethyltetraselenafulvalene, TMTSF, or the sulfur equivalent tetramethyltetrathiofulvalene, TMTTF). These stacks are aligned along the a-axis and separated in the c-direction by the anion X. Physical or chemical pressure, the latter is adjusted by the choice of the anion X, tune the properties of the $(TM)_2X$ salts. The temperature versus pressure phase diagram of these salts is universal [1–3], meaning that a compound under pressure has the same properties as another compound lying to his right on the phase diagram. At low pressures and high temperatures the $(TM)_2X$ salts are quasi-one-dimensional conductors. By lowering the temperature and increasing the pressure these salts cross over to a more two- and three-dimensional conductor. The ground state evolves under pressure through a spin-Peierls (SP), antiferromagnetic (AF), spin-density-wave (SDW), superconducting (SC) and metallic state. The mechanism responsible for superconductivity is still controversial. The hypothesis that AF-fluctuations could provide the attractive interaction has been supported by the vicinity of the superconducting state to a magnetically ordered state and a dependence between T_c and the strength of AF-fluctuations seen in resistivity experiments [3].

Pressures up to 6–10 GPa are needed to drive the sulfur compounds $(TMTTF)_2X$, located on the low pressure side, through the whole phase diagram. This wide range, which is not covered by the standard piston-cylinder cells, and the brittleness of the organics requiring excellent pressure conditions in order to obtain reliable measurements, are the reasons for which few high pressure studies on these compounds have been conducted. In $(TMTTF)_2BF_4$ an incomplete superconducting transition between 3.3 and 3.7 GPa has been reported by Auban-Senzier et al. [4]. We studied the high pressure phase diagram of $(TMTTF)_2BF_4$ by resistivity measurements, particularly to explore the possible relationships between the $T_c(p)$ behavior and characteristic features of the normal phase.

2 Experimental

Resistivity measurements were performed in a newly developped clamped Bridgman anvil cell adapted to liquid pressure mediums [5]. Daphne Oil 7373, which undergoes a vitrous transition at 1.9 GPa at ambient temperature [6], is used as pressure medium. The pressure is determined *in situ* by the superconducting transition temperature of lead. Due to the good pressure conditions, the full width of this transition (0–100% of the normal state resistance above T_c) can be as narrow as 7 mK corresponding to a pressure variation in the cell of 0.008 GPa. After numerous pressure increases the transition width broadens and the pressure gradient in the cell reaches up to 0.06 GPa. The pressure is changed at room temperature, where the resistivity ratio $R(p)/R(0)$ of the lead sample gives an alternative determination of the pressure. The pressure variation during cooling is less than 0.1 GPa.

This report focuses on the measurements performed on two $(TMTTF)_2BF_4$ needle shaped single crystals provided by P. Auban-Senzier (LPS, Université Paris-Sud, Orsay, France). The sizes of sample E21 and BP2 are $a \times b' \times c^\star = 0.5 \times 0.06 \times 0.036$ mm^3, respectively $0.87 \times 0.096 \times 0.072$ mm^3, where b' and $c^\star$ are the projections of

[a] e-mail: Anna-Sabina.Ruetschi@unige.ch

the b- and c-axis onto a rectangular parallelepiped. The a-axis resistivity is measured with a standard four probe dc method. Despite the anisotropic transport properties a homogeneous current injection is obtained by annular gold contacts evaporated onto the sample (P. Auban-Senzier). Annealed gold wires with a diameter of 10 μm are glued on these rings with Dupont conductor paste 4929N. The contact resistances vary considerably and range between 2 and 600 Ω at 4 K. These substantial resistances limit the measurement possibilities because the currents at low temperature needed to be kept below 50 μA to avoid Joule heating. The magnetic field is applied parallel to the c*-axis determined by the characteristic shape of the sample's cross-section. The two samples were measured in two different experiments. Sample E21 was measured at seven consecutive pressures ranging from 3.48 GPa to 6.51 GPa, and sample BP2 at thirteen pressures between 2.60 GPa and 5.93 GPa.

3 Results

At ambient conditions resistivities of different samples of a specific organic compound vary substantially. To better compare the two selected samples we have normalized the resistivity at 1 bar and 290 K of sample BP2 to the resistivity of sample E21, which equals 14 mΩ cm and is about three times lower than the one of BP2. During pressurisation changes in the geometric factor linking the resistance to resistivity can occur. Such changes appear us a sudden in- or decrease in the resistivity and have been corrected by taking the lower value as reference. Below 2 GPa the conductivity depends exponentially on p, which is a characteristic of the insulating regime. In the conducting regime σ increases linearly with p between 2 and 3 GPa and saturates at higher pressures.

Typical $\rho(T)$-curves of samples E21 and BP2 are shown in Figure 1. At low pressures $\rho(T)$ diminishes with temperature down to about 20 K. Below, an insulating phase develops which is suppressed with increasing pressure. A superconducting phase is found between 2.9 and 5 GPa with a maximum T_c of about 2 K. The main characteristics of the two selected samples are similar and both show large residual resistivity ratios indicating a good sample quality. However, for unknown reasons, resistivities differ noticeably at low temperature, especially in the pressure range of superconductivity. In the following two paragraphs the results of each sample are described in detail.

3.1 Sample BP2

At the lowest investigated pressure, 2.60 GPa, the resistivity shows two minima at $T_{min}^{high} = 17$ K and $T_{min}^{low} = 9$ K and increases by several orders of magnitude at lower temperatures, as shown in Figure 1. At 2.80 GPa the temperature of both minima decreases slightly. T_{min}^{low} is very shallow at 2.80 GPa and is no more visible at higher pressures. We refer therefore to T_{min}^{high} as T_{min} from now on. No sign of superconductivity is present down to about 500 mK at the two lowest pressures. At 2.91 GPa and below T_{min} the resistivity increases by more than two orders of magnitude before the appearance of a superconducting phase below $T_c^{90} = 1.06$ K. T_c^{90} is defined as the temperature, where the resistivity is 90% of the normal state value. This criterion will be used for the critical temperature, unless otherwise noted. For the first time in this compound, a zero resistance state (i.e. the resistivity drops below the measurement limit of 1 $\mu\Omega$ cm) is observed between 3.07 and 4.01 GPa (Fig. 2). The upper panel of Figure 3 shows the superconducting dome defined by various criteria of T_c. For all criteria, $T_c(p)$ has the usual asymmetric dome-like

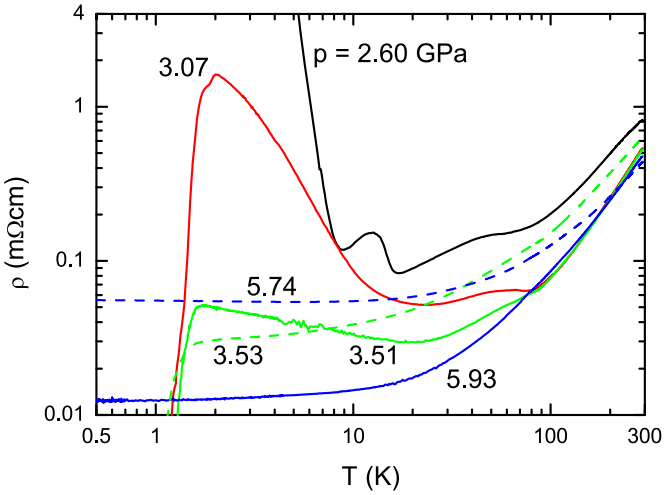

Fig. 1. Temperature dependence of the a-axis resistivity at different pressures. Solid lines represent data from sample BP2, dashed lines data from sample E21. Data at close pressures from different samples have the same color.

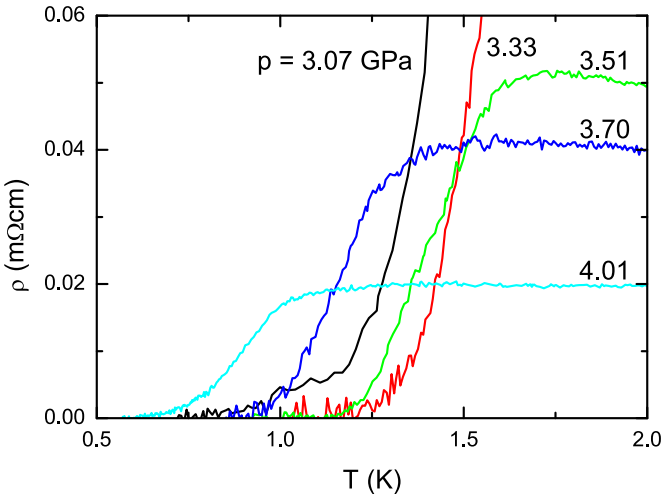

Fig. 2. $\rho(T)$-curves of sample BP2 at low temperature and different pressures. For the first time in $TMTTF_2BF_4$, zero resistivity is observed between 3.07 and 4.01 GPa.

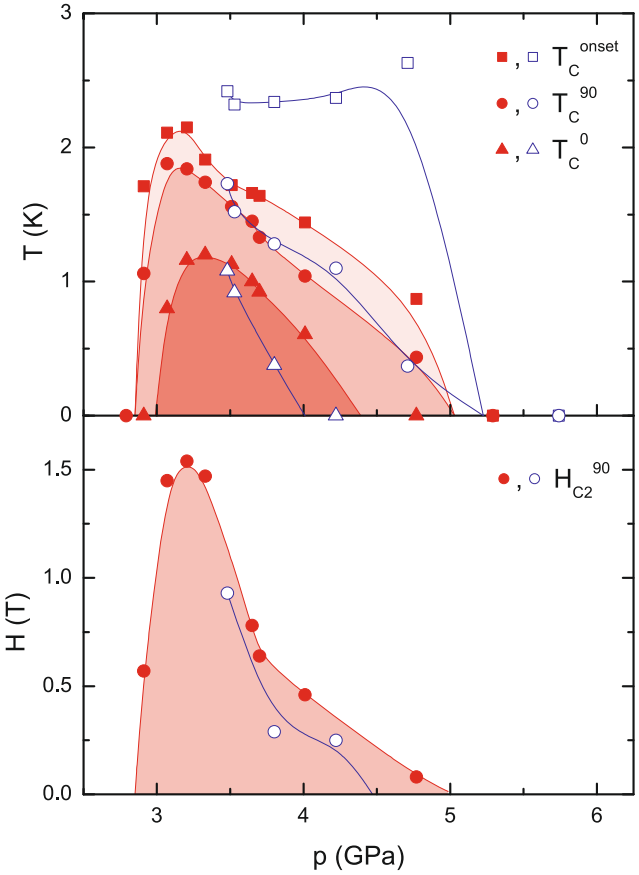

Fig. 3. Pressure dependence of the critical temperature (upper panel) and of the critical field (lower panel). Open symbols represent data from sample E21, closed symbols data from sample BP2. The lines are guides to the eye. The superconducting dome of sample BP2 is coloured.

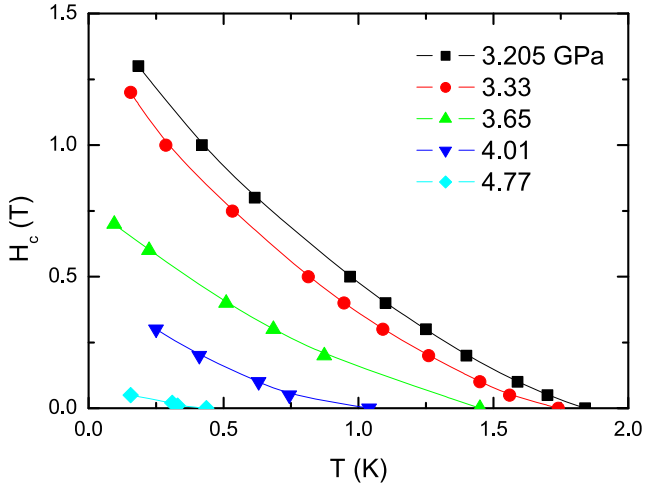

Fig. 4. Critical field of sample BP2 at various pressures. T_c is defined by the 90%-criterion. The lines are guides to the eye.

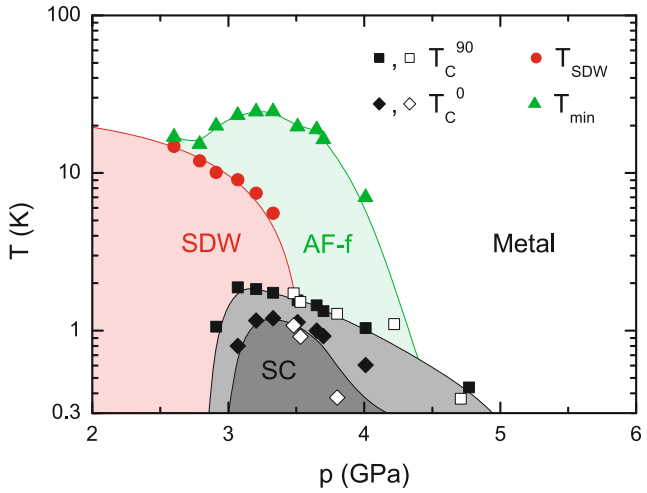

Fig. 5. Low temperature and high pressure phase diagram of $(TMTTF)_2BF_4$. Open symbols represent data from sample E21, closed symbols data from BP2. SDW, AF-f and SC stand for spin-density-wave, antiferromagnetic fluctuations and superconductivity respectively. The line delimiting the SDW-phase is a fit to the empirical formula given in the text. The other lines are guides to the eye.

shape, e.g. T_c strongly increases below T_c^{max} and slowly decays above. $T_c^{max} = 1.88$ K at $p = 3.07$ GPa. The transition width is broad and is minimal at 3.5 GPa. The superconducting phase disappears around 5 GPa.

Under a magnetic field, the resistivity has been measured down to about 50 mK. The critical field H_c, shown in the lower panel of Figure 3, is determined by the extrapolation of the $H_c(T)$-curves to $T = 0$. $H_c(p)$ has a similar dome shape as T_c with $H_c^{max} = 1.54$ T at 3.2 GPa. Above T_c^{max}, H_c first decreases rapidly to about 0.6 T at 3.7 GPa and then much slower at higher pressures. As shown in Figure 4, the $H_c(T)$-curves have a positive curvature at all pressures.

The transition temperature T_{SDW} into an insulating (spin-density-wave) state at low temperature is defined as the temperature of the second peak of the derivative $d(\ln \rho)/(d(1/T)$ vs. T for the two lowest pressures and as $\rho(T_{SDW}) = 2 \times \rho_{min}$ at higher pressures [7]. These two definitions give coincident results when both of them can be applied. T_{SDW} decreases from 14.8 K at 2.60 GPa to 5.6 K at 3.33 GPa, as shown in Figure 5. At higher pressures the SDW-phase is suppressed. All $\rho(T)$-curves show a pronounced minimum below 4 GPa. $T_{min}(p)$ is depicted in Figure 5. T_{min} increases from around 15 K to 25 K between 2.60 and 3.33 GPa and then decreases to 7 K at 4.01 GPa. The amplitude of the minimum decreases with pressure. We point out that $T_{min}(p)$ is usually not shown in the phase diagrams, with the exceptions of [2] and [3].

Around 60 K the temperature dependence of the $\rho(T)$-curves flattens and becomes even slightly negative at certain pressures. This feature clearly appears up to about 3.8 GPa and is also present in sample E21, albeit less pronounced. In Figure 1 the flattening is best seen in the $\rho(T)$-curves at 2.60 and 3.07 GPa. Above 4 GPa the $\rho(T)$-curves show a metallic behavior on the whole temperature range investigated. Between 4 and 5.29 GPa the resistivity

ratio increases from 27 to 40 due to a decrease in ρ_0. The lowest residual resistivity is 0.012 mΩ cm at 5.29 GPa, which is low for a sulfur compound.

After having reached the maximum load, the pressure was decreased. Superconductivity is reversible under pressure. T_c's of 0.76 K and 1.1 K are found at 5.2 GPa resp. 3.9 GPa. The transitions are not complete, probably due to the large pressure gradient of about 0.15 GPa, which could damage the sample. The $\rho(T)$-curves also show qualitatively the same behavior as on increasing the pressure, but the residual resistivities and the resistivities at room temperature are higher due to the deteriorated pressure conditions.

3.2 Sample E21

This sample has only been measured above about 3.5 GPa. As shown in Figure 3, T_c^{90} agrees well with the one of sample BP2. T_c^0 is suppressed more rapidly, but has qualitatively the same behavior as BP2. Surprisingly, T_c^{onset} is roughly independent of pressure. The critical field, shown in the lower panel of Figure 3, is slightly lower than in BP2, but the $H_c(T)$-curves show the same upward curvature as the former sample.

At the lowest investigated pressure (3.48 GPa) the $\rho(T)$-curve of sample E21 has a resistivity ratio of 8 and a minimum at $T_{min} = 7$ K. The resistivity increases by 10% before the transition into the superconducting phase. In contrast to sample BP2, at slightly higher pressure (3.53 GPa) there is no minimum in the $\rho(T)$-curve above T_c and the residual resistivity ρ_0 drops by a factor of two to 0.03 mΩ cm, thus increasing the resistivity ratio to 20. At this pressure the magnetoresistance has not been measured. Between 3.8 and 4.71 GPa the application of a magnetic field exceeding H_c reveals the presence of a very shallow minimum in the $\rho(T)$-curve below T_c^{onset}. Beyond the superconducting dome this minimum persists in zero field, which can be seen in Figure 7. T_{min} increases with pressure from 1.4 to 8 K. The amplitude of the minimum also increases with pressure, but remains small (5% at 6.51 GPa). Above 5 GPa the residual resistivity ρ_0 increases (Figs. 1 and 6). The origin of that and of the minimum at high pressures is unclear. No signs of a sample imperfection, such as cracks, appearing between 4.7 and 5.7 GPa were found. The lead manometer did not show any anomaly, which would indicate a deterioration of the pressure conditions due to an instability of the cell.

4 Discussion

4.1 The SDW-phase

The SDW-phase was only investigated with sample BP2. The strong pressure dependence of T_{SDW} close to the critical pressure p_c, at which T_{SDW} vanishes, is not a sign of a first order transition. In $(TMTSF)_2PF_6$, $T_{SDW}(p)$ could be measured down to the onset of superconductivity [9]. There, $T_{SDW}(p)$ has been found to follow a cubic pressure dependence. A fit of the $T_{SDW}(p)$ data from sample BP2 using the empirical formula given in [9], $T_{SDW}(p) = T_{SDW}(1\text{ bar}) - ((T_{SDW}(1\text{ bar}) - T_c)(p/p_c)^3)$, where $T_{SDW}(1\text{ bar})$ and p_c are free parameters and $T_c = 1.58$ K, yields a critical pressure $p_c = 3.49$ GPa at which the SDW is suppressed. A critical pressure of about 3.5 GPa is in good agreement with sample E21, where no more SDW-state is present at the first pressure of 3.48 GPa. Our fit reproduces values of T_{SDW} at lower pressures found by Auban-Senzier et al. [4]. Unlike $(TMTTF)_2PF_6$, where the critical pressure p_c coincides with the maximum of T_c^{onset}, the p_c in $(TMTTF)_2BF_4$ is at higher pressure than the maximum of the superconducting dome [2].

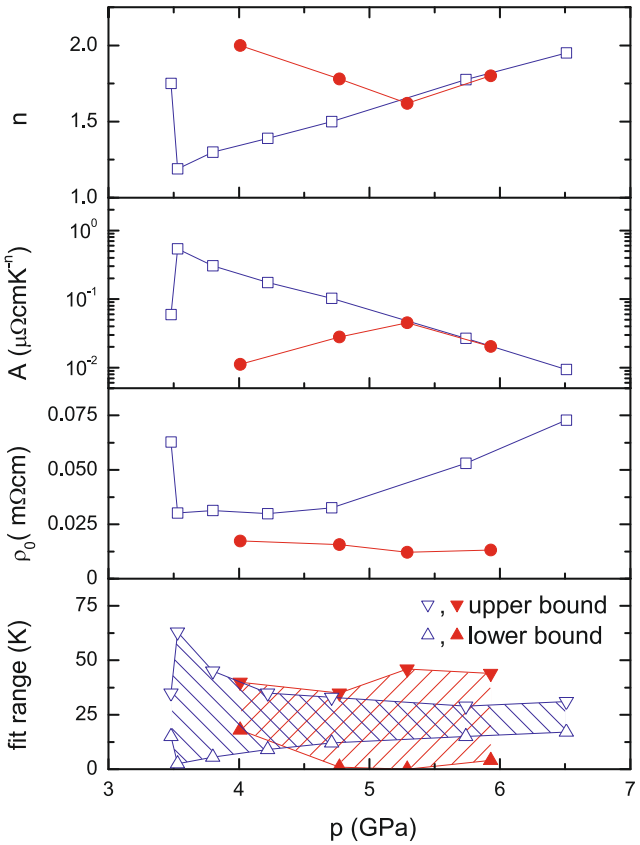

Fig. 6. Parameters of the fit $\rho(T) = \rho_0 + AT^n$ as a function of pressure. Open symbols represent data from sample E21, closed symbols data from sample BP2. The hatched areas in the lowest panel highlight the range of the fit. Quantum criticality is only shown by sample E21.

The critical pressure p_c of about 3.5 GPa, places $(TMTTF)_2BF_4$ about 1 GPa to the right of $(TMTTF)_2PF_6$ in the universal phase diagram [1–3]. This is in good agreement with the onset of superconductivity, which occurs around 4 GPa in $(TMTTF)_2PF_6$ and at 2.91 GPa in $(TMTTF)_2BF_4$.

At all pressures the transition into the SDW-state is broad and the $\rho(T)$-curves below T_{SDW} saturate at low temperature. Therefore they cannot be fitted to the law of thermally activated conduction ($\rho \sim \exp(\Delta/T)$). The

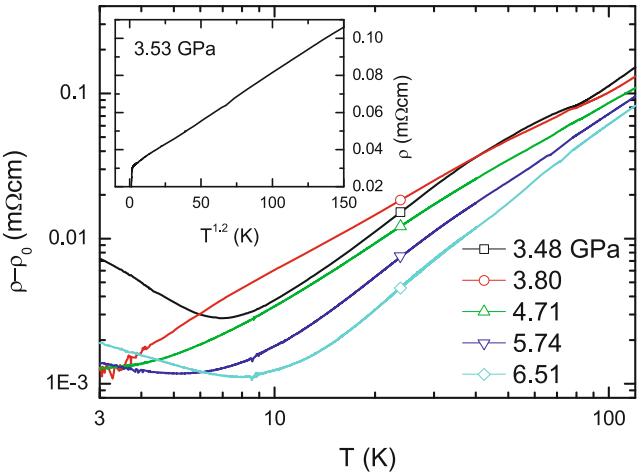

Fig. 7. Double logarithmic plot of $\rho - \rho_0$ of sample E21 as a function of temperature for different pressures. The inset shows the $\rho(T)$-curve at 3.53 GPa, which goes as $T^{1.2}$, in a linear plot.

saturation is due to a tendency for metallisation and is in agreement with a region found in $(TMTSF)_2PF_6$, where close to p_c the SDW-phase coexists with domains of a metallic or superconducting phase [9]. Evidence for a coexistence of superconductivity and SDW was also found in $(TMTTF)_2BF_4$ by critical current measurements [4]. Due to Joule heating of the sample we could not perform such measurements. An interesting feature is the occurence of two minimas in the $\rho(T)$-curve of BP2 at the two lowest pressures (Fig. 1). To our knowledge such an anomaly has not been seen before in a $(TM)_2X$ salt. It could be the sign of a strong competition between the metallic and the insulating state.

4.2 The superconducting phase

The superconducting phase of sample BP2 extends from 2.8 to 5.0 GPa. Above 3.07 GPa the superconducting domains in the sample are connected allowing a zero resistance state. The measurements performed on sample E21 cover only the region above T_c^{max} and confirm the upper pressure limit of the superconducting dome. A T_c^{max} of 2.15 K for the onset criterion is comparable to T_c's of other sulfur compounds.

Above T_c^{max}, $\partial T_c^{90}/\partial p = -0.09$ K/kbar for both samples, in good agreement with other organic compounds. The low pressure side of the superconducting dome is characterized by a steep increase of T_c from 0 K to about $0.6T_c^{max}$ in a pressure interval of 0.12 GPa. Measurements of ρ_a always yield steep slopes of $T_c(p)$, which can even be almost vertical as in $(TMTSF)_2PF_6$, where Vuletić *et al.* [9] report a jump in T_c from 0 K to nearly T_c^{max} for a pressure increase of only 0.2 kbar. A difference between samples BP2 and E21 is the onset of the superconducting transition. T_c^{onset} of sample BP2 follows the same pressure dependence as the other criteria for T_c, whereas T_c^{onset} of E21 is high and almost pressure independent (Fig. 3). Together with a faster decrease of T_c^0 in E21 this leads to a roughly two times wider transition in sample E21. Since the residual resistivity of sample E21 is higher than the one of BP2 and the resistivity ratio lower one could argue that sample E21 is less pure than BP2 and has thus the broader transition. It has been shown however that an increase in disorder not only broadens the transition but also lowers T_c [10], which does not happen in sample E21.

As shown in Figure 3, the maximum value of the critical field along $c^\star$, H_c, is 1.54 T and coincides with the highest T_c. The critical field in $(TM)_2X$-salts being much higher along the b'- and a-axis than along the $c^\star$-axis [16], this high value could indicate a misalignment of the sample. This is not the case, because similar values of H_c are found for both samples and a H_c of 1.5 T confirms previous measurements close to T_c^{max} in the title compound [4]. In the reentrant superconducting region, where insulating and conducting domains coexist, the field can enter the insulating domains, which results in a high H_c and could also explain the positive curvature of the H_c-curves (Fig. 4) [11]. Similar behaviors of the $H_c(T)$-curves for fields applied along $c^\star$ and high critical fields have been observed around T_c^{max} in $(TMTSF)_2PF_6$ for currents parallel to the a- or $c^\star$-axis [11,12]. Beyond p_c the superconducting phase is generally considered to be homogeneous [9]. Passing from the inhomogeneous to the homogeneous state, a strong decrease of H_c is expected. Indeed, H_c drops by a factor of two between 3.2 and 3.65 GPa. But in the whole superconducting phase the critical field remains large compared to the values in the homogeneous phase of other organic compounds (e.g. $H_c = 0.02$ T in $(TMTSF)_2PF_6$ [13], $H_c = 0.1$ T in $(TMTTF)_2Br$ and $(TMTSF)_2ClO_4$ [13,14]). Also, the positive curvature of the $H_c(T)$-curves remains up to at least 4 GPa. These findings are in contrast to the above cited studies ([11,12]), where at p_c or slightly above the critical field is reduced by more than a factor five to values below 0.2 T and where $H_c(T)$ has a rather linear temperature dependence. Our results could be the sign of insulating domains being present in the whole superconducting phase.

From the slopes of the $H_c(T)$-curves close to $T_c(H = 0)$ the parameter $(\xi_a(0)\xi_b(0))^{1/2}$ can be calculated using the Ginzburg-Landau relation $-dH_{c2}^{c^\star}/dT = \phi_0/(2\pi\xi_a(0)\,\xi_b(0)T_c)$, where ξ is the coherence length [15]. In the reentrant region, $(\xi_a(0)\xi_b(0))^{1/2} = 230$ Å, and increases to 430 Å at higher pressures. This latter value corresponds to about a quarter of the electron mean free path in the metallic state (with $\rho_0 = 0.012$ mΩ cm) and is in good agreement with the value found in $(TMTSF)_2ClO_4$ (≈480 Å) [16].

4.3 The fluctuation regime above T_c

Above the SDW respectively the superconducting phase, spin-fluctuations are present up to the temperature T_{min} defined by the minimum of the $\rho(T)$-curve. In $(TMTTF)_2PF_6$ the width in temperature of this region is largest at T_c^{max} and decreases with T_c [2,3]. This correlation between T_c and the spin-fluctuations has been interpreted as a strong evidence for a pairing mechanism

involving antiferromagnetic (AF) fluctuations. In sample BP2 a similar situation is found. Superconductivity appears at the same pressure at which T_{min} starts to increase. The highest T_{min} corresponds approximately to T_c^{max} and both regimes are suppressed with increasing pressure as shown in Figure 5. In sample E21 however the situation is very different. A minimum in the resistivity is present around 7 K at 3.48 GPa but disappears already at 3.53 GPa. Nevertheless, E21 has a similar T_c as BP2. These findings put a serious question mark on the correlations between AF-fluctuations and superconductivity and a pairing mechanism driven by such fluctuations. Minima in the $\rho(T)$-curve as high as 30 K in the pressure region around T_c^{max} have also been found in the title compound by Auban-Senzier [12].

We attribute the minimum in the $\rho(T)$-curve of sample E21 at 3.48 GPa to spin fluctuations, as in sample BP2. The very shallow minima appearing under a magnetic field at 3.8 GPa and being present up to 6.5 GPa probably have a different origin. Whereas at 3.48 GPa the resistivity increase is 10%, it is only 0.4% at 3.80 GPa. In addition ρ_0 drops by a factor two between 3.48 and 3.53 GPa and the temperature dependence of the resistivity below and above 3.5 GPa changes abruptly (see following discussion). Therefore the minima above 3.5 GPa seem not to be related to antiferromagnetic fluctuations. These very small upturns could be ascribed to the imperfect hydrostatic pressure conditions in the solidified Daphne oil[1].

In contrast to the above cited study on $(TMTTF)_2PF_6$, where T_{min} is a decreasing function of pressure [2,3], $T_{min}(p)$ has a maximum in sample BP2. The question needs to be addressed if the flattening in the $\rho(T)$-curves around 60 K, seen in Figure 1, influences the temperature of the minima in the resistivity curves and could be responsible for the maximum in $T_{min}(p)$. This possibility can be excluded because the minima in the resistivity curves at 2.9 and 3.5 GPa are at the same temperature, even though the flattening is much more pronounced in the lower pressure curve. The same happens for the resistivity curves at 2.8 and 3.7 GPa. The flattening of the $\rho(T)$-curves could be a reminiscence of the metal-semiconductor transition occuring around 200 K at ambient pressure. Under pressure this transition decreases to 60 K at 2.5 GPa [8].

4.4 Low temperature fits of ρ(T) and signs of quantum criticality

In the investigated pressure range the thermal expansion and the pressure coefficient of the samples are small, so that we can consider for our data that the measured constant pressure resistivity $\rho^p(T)$ is identical to the constant volume resistivity $\rho^v(T)$.

In the high pressure ($p > 3.5$ GPa) and low temperature ($T \lesssim 40$ K) region the resistivity is fitted to the law $\rho(T) = \rho_0 + AT^n$ usually followed close to a magnetic quantum critical point with $n < 2$. For $n = 2$, i.e. a Fermi liquid, the A coefficient is proportional to the square of the effective quasiparticle mass. Figure 6 shows the fitting parameters found for either sample. $\rho(T)$-curves of sample E21 are displayed in a double logarithmic plot in Figure 7. In the narrow pressure window between 3.48 and 3.53 GPa the n-coefficient of sample E21 drops from about 1.8 to 1.2 whereas the temperature coefficient A increases by one order of magnitude from 0.059 to 0.54 $\mu\Omega\,\mathrm{cm\,K}^{-n}$. From 3.53 to 6.5 GPa n increases linearly with pressure to about 2 and A decreases exponentially to 0.009 $\mu\Omega\,\mathrm{cm\,K}^{-n}$. At 3.53 GPa $\rho(T)$ is almost linear and the temperature range in which the fit is valid extends from the superconducting phase up to about 60 K (inset of Fig. 7). The fitting range is considerably smaller at the other pressures, partly due to the minimum in $\rho(T)$ which increases the lower bound. These behaviors strongly suggest a quantum critical point at the critical pressure $p_c = 3.5$ GPa, coinciding approximately with T_c^{max}. Towards the highest pressures the metallic state evolves into a conventional Fermi liquid. In another Fabre salt, $(TMTTF)_2AsF_6$, a similar temperature dependence of n is found [17]. There, close to the superconducting dome, n is also about 1 and increases to 1.5 at 10 GPa. The A-coefficient of about 0.5 $\mu\Omega\,\mathrm{cm\,K}^{-n}$ at the critical pressure, 3.5 GPa, is huge. At the maximum of T_c a similar value of A has been found in $(TMTTF)_2PF_6$ [18] and an even much higher value in $(TMTTF)_2AsF_6$ [17]. In the former compound, at pressures well above the superconducting dome, A decreased by about an order of magnitude.

Due to the larger expansion of the fluctuation regime in sample BP2 low temperature resistivity fits are only possible above 4 GPa. The n-coefficient is 2 at 4 GPa, decreases to 1.6 at 5.29 GPa and then increases to 1.8 at 5.93 GPa. In the same pressure intervals the A-coefficient increases from 0.011 $\mu\Omega\,\mathrm{cm\,K}^{-n}$ to 0.045 $\mu\Omega\,\mathrm{cm\,K}^{-n}$ and then decreases to 0.02 $\mu\Omega\,\mathrm{cm\,K}^{-n}$. At 4.01 GPa the lower bound of the fit range is high because of the minimum in $\rho(T)$ at 7 K. Beyond that pressure the fits extend down to much lower temperatures. At the two highest pressures applied to this sample, the n and A coefficients agree very well with the ones from sample E21, although the residual resistivity of sample E21 is four times higher. The different temperature dependence of the resistivities of the two samples below 4.8 GPa seems to be due to the much more developed AF-fluctuation regime of sample BP2, which masks the quantum critical behavior.

4.5 High temperature behavior

The $\rho(T)$-curves are also fitted to the power law T^n at high temperature. The fits extend from about 130 K to about 280 K. Sample BP2 follows roughly a T^2-law at all

[1] Resistivity measurements of the same compound have also been performed in a solid pressure medium (steatite). In this much less hydrostatic environment the resistivity has a metallic behavior only above about 150 K and below a very strong upturn of $\rho(T)$ is observed in the pressure range of about 4 to 9 GPa [5]. This suggests that pressure inhomogeneities can destroy the metallicity of the sample.

pressures (n varies between 1.9 and 2.2). E21 has a different behavior: n is 1.5 at 3.48 and 3.53 GPa, between 3.8 and 5.74 GPa n is constant around 1.75, and at 6.51 GPa n increases to 2. Below about 3.8 GPa the lower bound of the fits is restricted by the feature observed in the $\rho(T)$-curves around 60 K, which already diminishes the slope of the resistivity at considerably higher temperatures. But at all pressures a wide transition region between about 40 and 130 K separates the low and high temperature regimes, which cannot be fitted to a unique power law. In Fabre and Bechgaard salts a crossover from one dimension to two or three dimensions is observed by lowering the temperature at fixed pressure. The crossover temperature increases with pressure. In $(TMTTF)_2PF_6$ it is around room temperature at 3 GPa [19]. Since in the phase diagram $(TMTTF)_2BF_4$ is located about 1 GPa to the right of the former compound, one would expect no more one-dimensionality in the pressure and temperature range investigated in the present study. A conventional 3D Fermi liquid regime is characterized by a T^2 dependence of ρ along all crystallographic axes. Measurements of ρ_a alone are therefore not sufficient to determine the dimensionality of the sample. The T^2 dependence of ρ at all pressures in sample BP2 suggests however that in this sample a two- or three-dimensional behavior establishes at lower pressures than in sample E21, where the resistivity goes like T^2 only at 6.5 GPa. The high temperature n-coefficients can be compared to results found at ambient pressure in two different selenide compounds [20]. In $(TMTSF)_2PF_6$ the constant volume resistivity is proportional to $T^{0.56}$ and in $(TMTSF)_2ClO_4$, which is superconducting at ambient pressure, n is about 1.4, showing the expected evolution towards a Fermi liquid when going from the left to right side in the phase diagram.

The high temperature behavior of the two samples illustrates again that although different samples yield coincident results concerning the main phases like SDW and superconductivity a considerable disagreement exists between the samples in the more subtle features. A general characteristic of organic compounds is indeed the difficulty to distinguish their inherent properties from artefacts. This is specially a problem for high pressure experiments where the number of samples which can be measured is limited.

5 Conclusion

We investigated the high pressure phase diagram of $(TMTTF)_2BF_4$ by resistivity measurements on two high quality samples. Superconductivity extends from 2.9 to 5 GPa and a zero resistance superconducting state is found between 3 and 4 GPa. A high critical field and the positive curvature of the $H_c(T)$-curves up to at least 4 GPa could be interpreted by the presence of insulating domains not only close to the SDW-phase but throughout almost the entire superconducting dome. At temperatures above the superconducting transition the resistivity of each sample is different. One sample has an extended region of antiferromagnetic fluctuations characterized by a minimum in the $\rho(T)$-curves at temperatures as high as 25 K and extending well above the critical pressure p_c, where the SDW vanishes. In the other sample the minimum is suppressed at p_c. Low temperature power-law fits of the $\rho(T)$-curves of this latter sample show that at p_c the n-coefficient is minimal and close to 1 and the A-coefficient maximal. Furthermore, ρ_0 is low and the fit range maximal. These features could be the signature of a magnetic quantum critical point close to T_c^{max}.

Useful discussions with P. Auban-Senzier, D. Jérome, C. Bourbonnais and T. Giamarchi are acknowledged. We thank P. Auban-Senzier for providing us the samples and for the preparation of the annular gold contacts. This work was supported by the Swiss National Science Foundation.

References

1. D. Jérome, Science **252**, 1509 (1991)
2. D. Jaccard, H. Wilhelm, D. Jérome, J. Moser, C. Carcel, J.M. Fabre, J. Phys.: Cond. Matt. **13**, L89 (2001)
3. H. Wilhelm, D. Jaccard, R. Duprat, C. Bourbonnais, D. Jérome, J. Moser, C. Carcel, J.M. Fabre, Eur. Phys. J. B **21**, 175 (2001)
4. P. Auban-Senzier, C. Pasquier, D. Jérome, C. Carcel, J.M. Fabre, Synth. Met. **133**, 11 (2003)
5. A.-S. Rüetschi, D. Jaccard, Rev. Sci. Instrum. **78**, 123901 (2007)
6. T. Itou, K. Kanoda, K. Murata, T. Matsumoto, K. Hiraki, T. Takahashi, Phys. Rev. Lett. **93**, 216408 (2004)
7. R. Brusetti, M. Ribault, D. Jérome, K. Bechgaard, J. Phys. **43**, 801 (1982)
8. M. Tokumoto, T. Tani, K. Murata, T. Ukachi, H. Anzai, T. Ishiguro, Mol. Cryst. Liq. Cryst. **119**, 321 (1985)
9. T. Vuletić, P. Auban-Senzier, C. Pasquier, S. Tomić, D. Jérome, M. Héritier, K. Bechgaard, Eur. Phys. J. B **25**, 319 (2002)
10. N. Joo, P. Auban-Senzier, C.R. Pasquier, P. Monod, D. Jérome, K. Bechgaard, Eur. Phys. J. B **40**, 43 (2004)
11. I.J. Lee, P.M. Chaikin, M.J. Naughton, Phys. Rev. Lett. **88**, 207002 (2002)
12. P. Auban-Senzier, private communication
13. R. Greene, P. Haen, S.Z. Huang, E.M. Engler, M.Y. Choi, P.M. Chaikin, Molec. Crystals Liq. Crystals **79**, 183 (1982)
14. L. Balicas, K. Behnia, W. Kang, E. Canadell, P. Auban-Senzier, D. Jérome, M. Ribault, J.M. Fabre, J. Phys. I France **4**, 1539 (1994)
15. J.F. Kwak, R.L. Greene, W.W. Fuller, Phys. Rev. B **20**, 2658 (1979)
16. N. Toyota, M. Lang, J. Müller, *Low-Dimensional Molecular Metals* (Springer, Berlin, 2007)
17. M. Itoi, M. Kano, N. Kurita, M. Hedo, Y. Uwatoko, T. Nakamura, J. Phys. Soc. Jpn **76**, 053703 (2007)
18. C. Araki, M. Itoi, M. Hedo, Y. Uwatoko, H. Mori, J. Phys. Soc. Jpn **76**, Suppl. A, 198 (2007)
19. J. Moser, M. Gabay, P. Auban-Senzier, D. Jérome, K. Bechgaard, J.M. Fabre, Eur. Phys. J. B **1**, 39 (1998)
20. M. Dressel, K. Petukhov, B. Salameh, P. Zornoza, T. Giamarchi, Phys. Rev. B **71**, 075104 (2005)